https://doi.org/10.15407/ujpe70.9.620

A.V. ZINOVCHUK, V.S. SLIPOKUROV

- ¹ Ivan Franko State University of Zhytomyr
- (40, Velyka Berdychivska Str., Zhytomyr 10008, Ukraine; e-mail: zinovchuk.a@zu.edu.ua)
- 2 V.E. Lashkaryov Institute of Semiconductor Physics, Nat. Acad. of Sci. of Ukraine
- (41, Nauky Ave., Kyiv 03028, Ukraine)

AUGER RECOMBINATION IN POLAR InGaN/GaN QUANTUM WELLS

Auger recombination rate in polar $In_x Ga_{1-x}N/GaN$ quantum wells has been calculated in the framework of the full-band model. The key components of the model are the band structures of bulk binary nitrides (GaN and InN) obtained by the empirical pseudopotential method and the band structures of $In_x Ga_{1-x}N/GaN$ quantum wells (with various alloy compositions x) obtained by the linear combination of bulk bands. The dependence of the Auger recombination coefficients on the band gap, quantum well thickness, and carrier concentration has been calculated. The results obtained show that the band-gap dependences of the Auger coefficients for quantum wells are much weaker than in the case of bulk $In_x Ga_{1-x}N$ alloys. The dependence of the Auger coefficients on the quantum well width has a strong oscillatory character. At high carrier concentrations, a significant decrease in the Auger coefficients is observed, which we attribute to the influence of the Fermi statistics on the carrier population distribution over the quantum states.

Keywords: InGaN quantum wells, Auger recombination, polarization.

1. Introduction

Auger recombination in nitride compounds is of great importance; it is considered to be of the possible internal mechanisms responsible for the efficiency reduction of light-emitting devices based on InGaN/GaN quantum structures. Experimental confirmations of this assumption were obtained in works [1–3], where the detection of "hot" electrons excited by various types of Auger processes in the active region of InGaN/GaN light-emitting diodes (LEDs) was reported. Some quantitative experimental estimates of the Auger recombination coefficient in InGaN/GaN LEDs were made by comparing the measurement results for the differential carrier lifetimes and the results of calculations in the framework of the recombination coefficient model (the ABC-model) [4– 7]. These estimates demonstrate a rather large discrepancy among the obtained values for the Auger co-

Citation: Zinovchuk A.V., Slipokurov V.S. Auger recombination in Polar InGa/GaN Quantum Wells. $Ukr.\ J.\ Phys.$ 70, No. 9, 620 (2025). https://doi.org/10.15407/ujpe70.9.620. © Publisher PH "Akademperiodyka" of the NAS of Ukraine, 2025. This is an open access article under the CC BY-NC-ND license (https://creativecommons.org/licenses/by-nc-nd/4.0/)

efficients, which leads to further discussions about the importance of the Auger recombination in nitrides. In work [8], it was noted that the calculated values of the Auger recombination rate remain unexact, because it is experimentally difficult to distinguish various mechanisms of charge carrier loss without introducing additional phenomenological assumptions when interpreting the measurement results.

Besides experimental estimates, several calculations of the Auger recombination coefficients in nitrides were also performed. In early studies, bulk In-GaN compounds were mainly dealt with. Calculations of the rate of the direct Auger recombination mechanism predict a very strong dependence of the Auger coefficient on the band gap width in the InGaN compound [9, 10]. Indirect mechanisms with the participation of phonons were studied in the framework of perturbation theory [11] and second-order Fermi's golden rule [12].

Results concerning the influence of the disordered atomic structure of compounds on Auger recombination were presented in works [13, 14]. In bulk materials, the rate of Auger recombination is limited by the strict conditions of the simultaneous fulfillment

ISSN 2071-0194. Ukr. J. Phys. 2025. Vol. 70, No. 9

of the laws of energy and momentum conservation for charge carriers. In structures with reduced dimensionality, these conditions are relaxed. For example, in two-dimensional structures or quantum wells, momentum conservation is performed only for the component lying in the well plane. This circumstance affects the recombination rate rather strongly.

Furthermore, specifically for nitride quantum structures, another feature should be taken into consideration: the vast majority of such structures for emitting devices are grown along the polar crystallographic direction (c-direction) on sapphire substrates. It is known that the pseudomorphic growth in the c-direction leads to the appearance of strong spontaneous and piezoelectric polarization fields [15], which can affect the Auger recombination rate.

Most calculations of the Auger recombination rate in InGaN/GaN quantum wells are based on the kp-model of the band structure in the envelope-function approximation [16–18]. The results of works [17, 18] show that the Auger recombination rate is high enough to explain the drop in the efficiency in nitride LEDs. However, the calculations of work [16] predict the values for the Auger recombination rate that are much lower than those obtained in works [17,18]. One of the reasons for this discrepancy may be the limiting character of kp-models: they adequately describe only the edges of energy bands, whereas, during recombination processes, the carriers also move to highenergy states that lie far from the band edges.

To overcome the problems with kp-models, the full-band structure (the empirical pseudopotential method) was used in work [19]. The results of this calculation give an Auger coefficient value for In-GaN quantum wells that is comparable to the values predicted by calculations for indirect processes in bulk InGaN compounds [11]. However, in work [19], the polar properties of nitride structures were not taken into account, and attention was focused only on the quantum well with the composition x=0.25 (In_{0.25}Ga_{0.75}N/GaN).

One of the latest works on this topic was based on a completely atomistic description of the recombination process [20]. The computational model of this work can make allowance for the influence of local fluctuations in the arrangement of indium atoms in the quantum well on the recombination rate. The presented results showed that various configurations of the arrangement of indium atoms in the quantum well

with a fixed content x lead to random deviations of the Auger recombination rate within an interval from 10^{-32} to 10^{-29} cm⁶s⁻¹, which is too large, taking the available experimental data into account.

Therefore, further studies of Auger recombination in $\text{In}_x\text{Ga}_{1-x}\text{N}/\text{GaN}$ quantum wells are needed in order to understand the role of Auger transitions in light-emitting devices. This is especially true for quantum wells with high In contents (x>0.5), which have recently started to be applied in red-emitting LEDs [21] and for which there are no theoretical estimates of the Auger recombination rate at all.

In this work, we will calculated the rate of the direct Auger process in polar $In_xGa_{1-x}N/GaN$ wells with various In contens x from 0.1 to 0.6. This process corresponds to optical transitions from the violet to the red part of the visible spectrum. Our model is based on the energy band structure of quantum wells that was obtained using the method of linear combination of full bulk bands of binary GaN and InN compounds, which, in turn, were described by means of the empirical pseudopotential method.

2. Theoretical Model

According to the method of linear combination of bulk bands, the wave function in systems with reduced dimensionality is represented as a superposition of Bloch functions of the bulk materials entering the systems. In work [22], it was shown that, for 2D systems of the quantum-well type, the correct choice of basis Bloch functions for the representation is quite important. With the proper choice, the Schrödinger equation for the desired wave function of a 2D structure in the Bloch function basis represents a separate problem of finding eigenvalues for every wave vector belonging to the two-dimensional Brillouin zone of the system. That is, the vector can be considered a "quantum number" that "enumerates" quantum states in the 2D structures.

For a polar ${\rm In}_x{\rm Ga}_{1-x}{\rm N}/{\rm GaN}$ quantum well grown along the z-direction of real space, the Schrödinger equation in the bulk Bloch function representation looks like

$$\langle n(\mathbf{k}, k_z) | H | n'(\mathbf{k}, k_z') \rangle =$$

$$= \frac{2\pi}{L_z} \sum_{n', k_z'} E_{\text{Bulk}}^{(n)}(\mathbf{k}, k_z) \, \delta_{k_z, k_z'} \delta_{n, n'} +$$

$$+ \sum_{G_z} U(k_z' + G_z - k_z) \langle u_{n(\mathbf{k}, k_z - G_z)} | u_{n'(\mathbf{k}, k_z')} \rangle, \qquad (1)$$

where $E_{\mathrm{Bulk}}^{(n)}(\mathbf{k},k_z)$ is the energy associated with the Bloch function $|n(\mathbf{k},k_z)\rangle$ of the bulk material, k_z is the component of the wave vector along the quantization direction, \mathbf{k} is the wave vector in the 2D Brillouin zone, $U(k_z)$ is the Fourier transform of the quantum confinement potential, $\langle u_{n(\mathbf{k},k_z-G_z)}|u_{n'(\mathbf{k},k_z')}\rangle$ is the overlap integral between the periodic parts of Bloch functions, L_z is the quantum structure length associated with periodic boundary conditions, and G_z is the z-component of those vectors in the reciprocal lattice of bulk materials that have a zero component in the plane parallel to the quantum well, $\mathbf{G}=(0,G_z)$.

In the 2D systems, the periodicity of the crystal lattice potential is broken only in the zdirection. Therefore, the quantum confinement potential depends only on one spatial coordinate, z. As a result, the Fourier transform of the potential is also a function of only the k_z component of the wave vector. Summation in Eq. (1) is performed over a discrete set of wave vectors k_z' -components and the bulk-band numbers n'. The k_z -set must satisfy the condition $k_z \neq k_z' + G_z$ for all G_z . In the case of nitrides with a wurtzite-type crystal lattice, $G_z = \pm 2\pi/c$, where c is the lattice constant in the polar direction. Therefore, the k'_z -values belong to the interval $[-\pi/c, \pi/c]$. As was already noted, the vectors \mathbf{k} must belong to the 2D Brillouin zone. For polar $In_xGa_{1-x}N/GaN$ quantum wells, this is a hexagon lying in the base of the 3D Brillouin zone of bulk nitrides.

For each chosen **k**-vector, the basis of the representation $|u_{n'(\mathbf{k},k_z')}\rangle$ was chosen by uniformly dividing the discretization interval $[-\pi/c;\pi/c]$: $k_{z,i}=i\pi/(N_{k_z}c)$ ($i\in[-N_{k_z},N_{k_z}]$). In essence, the number N_{k_z} specifies the dimensionality of the representation basis. The number of bulk Bloch functions included into the basis is equal to $(N_{k_z}+1)n_b$, where n_b is the number of the bulk bands (enumerated by the numbers n') included into calculations.

Since the studied $\text{In}_x \text{Ga}_{1-x} \text{N}$ quantum wells were embedded into the matrix of bulk GaN, the quantities $E_{\text{Bulk}}^{(n)}(\mathbf{k},k_z)$ and $|n(\mathbf{k},k_z)\rangle$ were considered as the energies and the Bloch functions, respectively, for bulk GaN. To determine them, we used the empirical pseudopotential method with an optimized form of pseudopotentials in order to achieve a correspondence to the currently known experimental data and the results of first-principles calculations for the band structure of binary nitrides with the wurtzite lattice [14].

The quantum structure length L_z (or the periodicity length) should be much larger than the quantum well thickness d_{QW} in order to minimize the influence of boundary effects. According to the choice of the representation basis, $L_z = 2N_{k_z}c \gg d_{\rm QW}$. The latter inequality imposes a restriction on the minimum allowable dimensionality of the representation basis N_{k_z} . Our test calculations showned that, for example, if $d_{\rm OW} = 2.0$ nm, stable results can be achieved at $N_{k_z} = 31$ and the number of bulk bands $n_b = 2$ (the lowest two conduction bands) when calculating the electron quantum states or $n_b=6$ (the highest six valence bands) when calculating the hole quantum states. Larger N_{k_z} -values increase the computational load, but do not lead to a noticeable improvement in the result quality.

Summation over G_z in Eq. (1) was performed only over the three smallest vectors $\mathbf{G} = (0, G_z)$ of the reciprocal lattice. The energies and the wave functions of charge carriers in the quantum well for a given wave vector \mathbf{k} were obtained by diagonalizing the Hamiltonian matrix from Eq. (1) using the functions from the linear algebra package LAPACK.

The quantum confinement potential U(z) was obtained using an iterative algorithm for the selfconsistent solution of the system of Schöer-Poisson equations [23]. The input parameters of the algorithm were the quantum well thickness d_{OW} , the carrier concentrations in the well, and the barriers, and the quantum well depth Δ . The parameter Δ was determined by the well composition x and the band gap at the $GaN/In_xGa_{1-x}N$ heterointerface, which was taken to equal $\Delta E_c/\Delta E_v = 70:30$ [24]. The quantum well was arranged between two GaN barriers of the nand p-types with the constant bulk charge carrier concentrations $n_{br} = 10^{17} \text{ cm}^{-3} \text{ and } p_{br} = 10^{17} \text{ cm}^{-3}$, whereas the surface concentrations of electrons (n)and holes (p) in the well were varied within an interval from 10^{10} to 10^{14} cm⁻⁴ to study their effect on the recombination rate.

Due to the polar nature of nitrides, surface charges arise at the heterointerfaces between the well and the barriers. They were taken into account as an additional component in the Poisson equation. In the general case, these charges arise as a result of both spontaneous and piezoelectric polarization. However, due to a very small difference between the values of the spontaneous polarization constants for GaN and InN, the surface charge magnitude is mainly determined by

the piezoelectric response [15]. Provided the pseudomorphic growth along the polar direction, the piezoelectric response to a biaxial strain in the (0001) plane is expressed as $P_z = 2\epsilon_{xx}(e_{31} - e_{33}C_{13}/C_{33})$, where e_{31} and e_{33} are the piezoelectric tensor components, C_{31} and C_{33} are the stiffness tensor components, and $\epsilon_{xx} = (a_{\text{GaN}} - a_{\text{InGaN}})/a_{\text{InGaN}}$ is the component of the strain tensor in the quantum well plane. Numerical values for the lattice, elastic, and piezoelectric parameters of $\text{In}_x \text{Ga}_{1-x} \text{N}$ were determined via the linear interpolation between the corresponding values for binary compounds [25–27].

At the first stage, the energy band structure of the quantum well was calculated, with the model of an ordinary rectangular well with a finite depth taken for the quantum confinement potential in the initial approximation. Then, the Fermi quasi-levels were determined for the given surface concentrations of electrons and holes in the well. The Fermi quasi-levels were calculated using numerical integration of the Fermi distribution functions over the 2D Brillouin zone. To reproduce typical conditions of electrical injection of charge carriers in LEDs, it was assumed that the surface concentrations of electrons and holes in the well are equal, n = p. This equality leads to the splitting of the corresponding Fermi quasilevels. Using the approximation of constant (coordinate-independent) Fermi quasi-levels, the electric potential values for the quantum confinement at the quantum structure boundaries were obtained, which were used as boundary conditions for the numerical solution of the Poisson equation. To speed up the self-consistent algorithm and prevent unphysical solutions, the linearization procedure was applied to the Poisson equation according to the scheme presented in work [23]. The obtained potential was substituted into Eq. (1), and its solution gave a second approximation for the band structure of the quantum well. Then, new Fermi quasi-levels and a new form of the quantum confinement potential were calculated. This procedure was repeated until the selfconsistency was achieved.

Next, we proceed directly to Auger recombination, whose rate can be calculated as follows:

$$\begin{split} R_{n(p)} &= 2\frac{2\pi}{\hbar}\frac{A^3}{(2\pi)^6}\int\!\!\!\int\!\!\!\int\!\!\!\int |M(\mathbf{k}_1,\mathbf{k}_2,\mathbf{k}_{1'},\mathbf{k}_{2'})|^2 \times \\ &\times f_{n(p)}(E_1)f_{n(p)}(E_2)f_{p(n)}(E_{1'})(1-f_{n(p)}(E_{2'})) \times \\ &ISSN~2071\text{-}0194.~Ukr.~J.~Phys.~2025.~Vol.~70,~No.~9 \end{split}$$

$$\times (1 - \exp[(E_{\mathrm{F}p} - E_{\mathrm{F}n})/k_b T]) \times \times \delta(E_1 + E_2 - E_{1'} - E_{2'}) \times \times \delta(\mathbf{k}_1 + \mathbf{k}_2 - \mathbf{k}_{1'} - \mathbf{k}_{2'}) d\mathbf{k}_1 d\mathbf{k}_2 d\mathbf{k}_{1'} d\mathbf{k}_{2'},$$
(2)

where the subscript n denotes the rate of the e-e-h process, and the subscript p the rate of the h-h-e process; $|M|^2 = |M_{\text{dir}}|^2 + |M_{\text{ex}}|^2 - |M_{\text{dir}} - M_{\text{ex}}|^2$, where M_{dir} and M_{ex} are the direct and exchange matrix elements of Coulomb interaction; $f_n(E)$ and $f_p(E)$ are the Fermi–Dirac functions; $E_{\text{F}n}$ and $E_{\text{F}p}$ are the electron and hole Fermi quasi-levels; the subscripts 1, 2 and 1', 2' denote the initial and final states of recombining carriers; and A is the quantum well area. To calculate $|M|^2$ in the basis of bulk Bloch functions, we followed the procedure described in work [28] and used a simple static model of Coulomb interaction screening with the high-frequency dielectric permittivity ($\epsilon_{\infty} = 5.5$) and a 2D analog of the Debye screening length [29].

Integration in Eq. (2) was carried out over all possible initial and final states of the particles, which actually meaned the fourfold (reduced to threefold, due to the presence of delta function) integration over the 2D Brillouin zone. We performed such integration using the Monte Carlo method. To improve the convergence of the numerical integration process, we confined the integration region to only those parts of the 2D Brillouin zone, where the product of the Fermi–Dirac functions in Eq. (2) was not small, i.e., the initial states of recombining particles belonged only to small parts of the 2D Brillouin zone near the ground state. The size of those parts was determined using preliminary test calculations.

Making allowance for the e-e-h and h-h-e processes, the total Auger recombination rate per unit area of the quantum well can be written as $R = R_n + R_p =$ $=C_n n^2 p + C_p p^2 n$, where n and p are the surface electron and hole concentrations, and C_n and C_p are the 2D Auger coefficients for the e-e-h and h-h-eprocesses, respectively. Assuming the equality of the surface electron and hole concentrations in the well, the recombination rate can be written as $R = Cn^3$. where $C = C_n + C_p$. Standard 3D Auger coefficients, which are often used when modeling recombination and transport processes in nitride quantum structures, as well as when interpreting the corresponding experimental results, can be calculated from the results presented in this paper for 2D analogs using the relationship $C_{3D} \approx C d_{\text{QW}}$.

3. Results

All calculations in this work were performed for the temperature $T=300~{\rm K}$ and assuming the equal electron and hole concentrations in the well. Three calculation stages were carried out to study the following dependences of the Auger coefficients: on the effective band gap width E_g in the quantum well, the quantum well thickness $d_{\rm QW}$, and the charge carrier concentration n.

At the first stage, we calculated the Auger recombination rate in quantum wells with the indium atom content varying from x=0.1 to 0.6 at the fixed well thickness $d_{\rm QW}=2.0$ nm and the fixed charge carrier concentration $n=10^{12}~{\rm cm}^{-2}$. The calculation

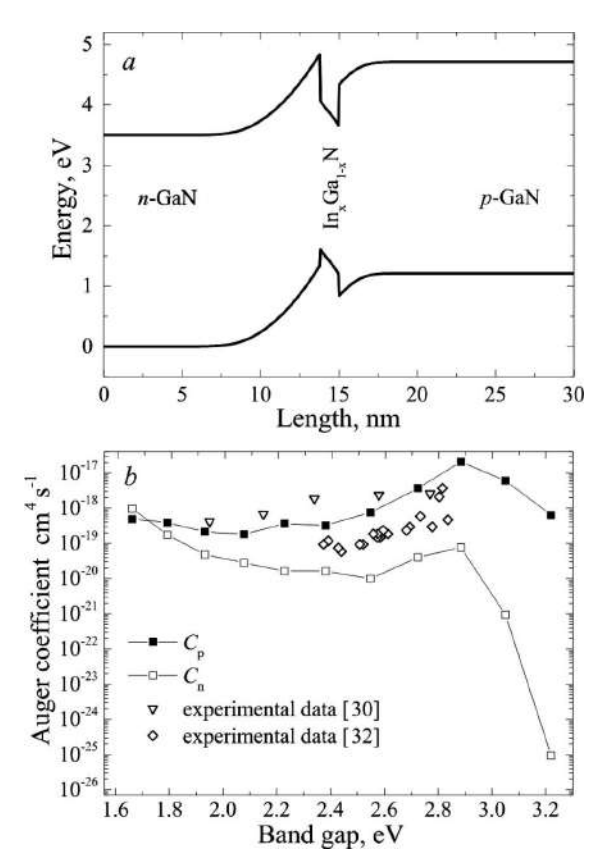


Fig. 1. (a) Quantum confinement potential for a polar $\ln_x \text{Ga}_{1-x} \text{N}/\text{GaN}$ quantum well with x=0.3 obtained as a result of a self-consistent solution of the Schrödinger–Poisson equations. (b) Dependences of the Auger coefficient for the e-e-h $(C_n$, hollow squares) and h-h-e $(C_p$, solid squares) processes on the band gap width for polar $\ln_x \text{Ga}_{1-x} \text{N}/\text{GaN}$ quantum wells (x=0.1-0.6) with $d_{\text{QW}}=2.0$ nm at T=300 K and $n=10^{12}$ cm⁻². For comparison, experimental results from works [30, 32] are shown

showed that, at $d_{\rm QW}{=}2.0$ nm, the variation of the In content x from 0.1 to 0.6 gives rise to the creation of quantum wells with effective band gap widths corresponding to optical transitions with energies from $E_g=1.8$ to 3.2 eV, i.e., covering the entire visible spectral interval.

Figure 1 illustrates the dependences of the Auger coefficients on E_g for the processes e-e-h (C_n) and h-h-e (C_p) . As can be seen from Fig. 1, for all wells with $E_g > 2.0$ eV, the process h-h-e dominates over the process e-e-h $(C_p > C_n)$. Only for quantum wells with a high content of indium atoms (they correspond to the red wing of the visible spectrum), both processes are of the same order. This result testifies that the widely used assumption about the leading role of the e-e-h process in light-emitting devices based on $\text{In}_x \text{Ga}_{1-x} \text{N}/\text{GaN}$ is not justified. An analysis of the efficiency of light-emitting devices based on the recombination coefficient model should include the total Auger coefficient $C = C_n + C_p$, which is mainly determined by the rate of the h-h-e process.

The dependence of C_p on E_g has a peak of $C_p = 1.9 \times 10^{-17}$ cm⁴c⁻¹ at $E_g = 2.9$ eV. When the bandgap width decreases from 2.9 to 2.6 eV (the violet-blue section in the visible spectrum), a reduction of C_p to $C_p = 6.5 \times 10^{-19}$ cm⁴c⁻¹ is observed, whereas, for all $E_g < 2.6$ eV (the green-red section of the visible spectrum), C_p has approximately the same value $C_p \approx 2.5 \times 10^{-19}$ cm⁴s⁻¹. This trend is consistent with experimental estimates of the Auger coefficient in nitrides obtained from the measurements of the differential lifetime of charge carriers [30, 31] and the photoluminescence kinetics [32].

It should be noted that these experimental data cannot be reproduced by modeling Auger recombination in bulk nitrides. Theoretical estimates based on various models [11, 13] predict a monotonically increasing Auger coefficient when going from widegap to narrow-gap quantum wells. Such a comparison proves that quantum confinement and polarization fields substantially affect the recombination process, so, estimates based on bulk models may give incorrect results.

At the second stage of our study, the dependence of the Auger coefficients on the quantum well thickness $d_{\rm QW}$ was calculated for the fixed In content x=0.3 ($E_g=2.6~{\rm eV}$) and the fixed charge carrier concentration $n=10^{12}~{\rm cm}^{-2}$. The calculations were performed for the thickness $d_{\rm QW}$ varying from 1.5 to 5.5 nm. As

can be seen from Fig. 2, a, for both the e-e-h and h-h-e processes, the dependence of the Auger coefficients on the well thickness has an oscillatory character.

As was noted in work [33], the dependence of the recombination rate on the well thickness is considerably determined by the final state, bound (a discrete energy spectrum) or unbound (a continuous energy spectrum), in which the particle is after recombination. For the nitride quantum wells considered in this work, the effective band gap width was significantly larger than the well depth for both electrons and holes for all x from 0.1 to 0.6. Therefore, the final states of Auger processes in nitride quantum wells are unbound.

The analysis of the Auger recombination rate for such transitions is determined mainly by the discreteness of the hole energy spectrum because of the complicated structure of the valence band in binary nitrides. The discreteness of the spectrum, in turn, is directly determined by the quantum well thickness. Due to the spectrum discreteness, the conservation of the energy of recombining particles (the energy delta function in Eq. (2)) is satisfied only for a limited number of transitions. In addition, transitions from some of those discrete levels into the continuous final spectrum are forbidden by the selection rules for the matrix element of Coulomb interaction. Such selection rules arise from the necessity to preserve the symmetry of the particle wave functions before and after recombination. Thus, at certain well thicknesses, the quantum confinement potential can reduce the recombination rate due to the restrictions imposed by the aforementioned selection rules. In the case of transitions to bound states, the selection rules generally make the matrix element of Coulomb interaction equal to 0, and the recombination rate at certain well thicknesses drops sharply. However, in the case of transitions to unbound states, such a sharp decrease does not occur, since the electron or the hole in the final state is scattered onto high-energy levels, which are strongly extended beyond the quantum well boundaries [34, 35].

At the last stage of the work, we calculated the dependence of the Auger coefficients on the surface carrier concentration for the fixed In content x=0.3 ($E_g=2.6$ eV) and the fixed quantum well thickness $d_{\rm QW}=2.0$ nm. The results showed that the Auger coefficients are almost independent of the carrier concentration at $n<10^{12}$ cm⁻². However, with an in-

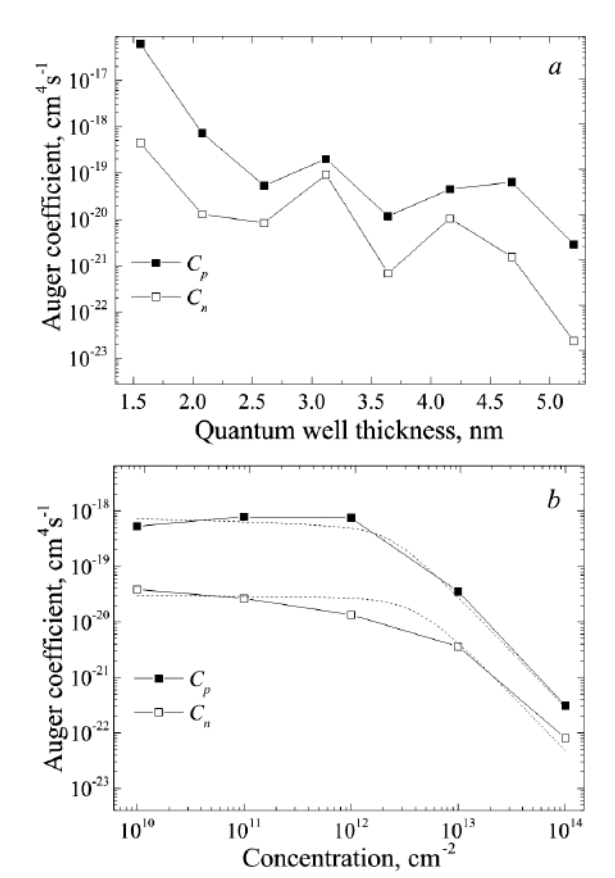


Fig. 2. Dependences of the Auger coefficient for the e-e-h (C_n , hollow squares) and h-h-e (C_p , solid squares) processes in polar $\ln_x \mathrm{Ga}_{1-x} \mathrm{N}$ quantum wells with x=0.3 at T=300 K (a) on the quantum well thickness d_{QW} for the carrier concentration $n=10^{12}$ cm⁻² and (b) on the carrier concentration $n=10^{12}$ cm⁻² and (b) on the carrier concentration $n=10^{12}$ cm⁻² and (b) demonstrate the approximation results for the obtained dependences using the formula $C=C_0/(1+n^2/n_0^2)$ (for the e-e-h process, $C_0=3.0\times 10^{-20}$ cm⁴s⁻¹ and $n_0=4.0\times 10^{12}$ cm⁻⁴; for the h-h-e process, $C_0=7.2\times 10^{-19}$ cm⁴s⁻¹ and $n_0=2.0\times 10^{12}$ cm⁻⁴)

crease of concentration, $n > 10^{12}$ cm⁻², both C_p and C_n begin to decrease quite substantially. We associate this reduction with the filling of quantum states, i.e., this if the influence of Fermi statistics on the recombination process. The Auger recombination rate is directly proportional to the cube of the charge carrier concentration only if the distribution of carriers over the quantum states is described by the classical Boltzmann statistics.

At high concentrations, the energies of Fermi quasilevels are so close to the band edges that the classical approximation is no longer applicable. In this case, the Auger recombination rate has a subcubic dependence on the charge carrier concentration. However, when dealing with phenomenological models describing the efficiency of light-emitting devices, it is convenient to retain the cubic dependence of the Auger recombination rate and account for the effect of quantum state filling using the Auger coefficient that depends on the concentration. An obvious assumption is to consider this dependence as an inverse proportionality, $C = C_0/(1 + n/n_0)$, where C_0 and n_0 are fitting parameters [4]. However, an analysis of our results showed that both C_n and C_p decrease with the concentration more rapidly and cannot be approximated by the above formula with a sufficient accuracy. The calculated dependences of the Auger coefficients on concentration are quite adequately described by the formula $C = C_0/(1+n^2/n_0^2)$. The best match was observed at $C_0 = 3.0 \times 10^{-20} \text{ cm}^4 \text{s}^{-1}$ and $n_0 = 4.0 \times 10^{12} \text{ cm}^{-4} \text{ for the } e\text{-}e\text{-}h \text{ process, and at } C_0 = 7.2 \times 10^{-19} \text{ cm}^4\text{c}^{-1} \text{ and } n_0 = 2.0 \times 10^{12} \text{ cm}^{-4}$ for the h-h-e process (which dominates at all considered carrier concentrations). Such a quadratic reduction of the Auger coefficients suggests that the Auger recombination rate in nitride quantum wells becomes an almost linear function of the concentration when transiting into the degenerate case. Under such circumstances, the following question arises again: "Is the Auger recombination the main cause of the reduced efficiency of light-emitting devices based on nitride quantum wells?"

4. Conclusions

In this work, we have performed a numerical simulation of the Auger recombination rate in polar $In_xGa_{1-x}N/GaN$ quantum wells. The computational model is based on the full energy band structure of the quantum wells, which is obtained using the method of linear combination of bulk bands. The results show that, under typical conditions of electrical injection of charge carriers into light-emitting devices, the Auger recombination rate is mainly determined by the h-h-e process for all In contents x from 0.1 to 0.6. This result calls into question the widely held assumption about the dominant role of the e-e-h process in $In_xGa_{1-x}N/GaN$ -based light-emitting devices. The application of the coefficient C_n , when analyzing the efficiency of light-emitting devices in

the framework of phenomenological models for recombination coefficients substantially underestimates the Auger recombination rate and can lead to an incorrect interpretation of experimental results. The dependence of the Auger coefficients on the effective band gap width of the quantum well turned out much weaker than in the case of bulk nitride compounds, which is a consequence of the strong influence of the quantum confinement and polarization fields on the recombination process. The studies have shown that the Auger recombination rate is directly proportional to the cube of the charge carrier concentration $(R \sim n^3)$ in the quantum well only for the concentrations not exceeding 10^{12} cm⁻². At higher concentrations, the cubic dependence of the Auger recombination rate gradually transforms into an almost linear one $(R \sim n)$; we associate this change with the filling of quantum states. In this work, we have considered only direct Auger recombination processes. However, additional calculations revealing the role of indirect processes (involving phonons or atomic disorders) would be very interesting for elucidating the influence of Auger recombination on the quantum efficiency of light-emitting devices based on InGaN quantum wells.

- J. Iveland, L. Martinelli, J. Peretti, J. S. Speck, C. Weisbuch. Direct measurement of Auger electrons emitted from a semiconductor light-emitting diode under electrical injection: Identification of the dominant mechanism for efficiency droop. *Phys. Rev. Lett.* 110, 177406 (2013).
- M. Binder, B. Galler, M. Furitsch, J. Off, J. Wagner, R. Zeisel, S. Katz. Investigations on correlation between I-V characteristic and internal quantum efficiency of blue (AlGaIn)N light-emitting diodes. Appl. Phys. Lett. 103, 221110 (2013).
- D.J. Myers, A.C. Espenlaub, K. Gelzinyte, E.C. Young, L. Martinelli, J. Peretti, C. Weisbuch, J.S. Speck. Evidence for trap-assisted Auger recombination in MBE grown InGaN quantum wells by electron emission spectroscopy. Appl. Phys. Lett. 116, 091102 (2020).
- A. David, M.J. Grundmann. Droop in InGaN lightemitting diodes: A differential carrier lifetime analysis. Appl. Phys. Lett. 96, 103504 (2010).
- B. Galler, P. Drechsel, R. Monnard, P. Rode, P. Stauss, S. Froehlich, W. Bergbauer, M. Binder, M. Sabathil, B. Hahn, J. Wagner. Influence of indium content and temperature on Auger-like recombination in InGaN quantum wells grown on (111) silicon substrates. Appl. Phys. Lett. 101, 131111 (2012).
- A. David, N.G. Young, Ch.A. Hurni, M.D. Craven. Alloptical measurements of carrier dynamics in bulk-GaN

- LEDs: Beyond the ABC approximation. Appl. Phys. Lett. 110, 253504 (2017).
- F. Nippert, S.Yu. Karpov, G. Callsen, B. Galler, Th. Kure,
 C. Nenstiel, M.R. Wagner, M. Strasburg, H.-J. Lugauer,
 A. Hoffmann. Temperature-dependent recombination coefficients in InGaN light-emitting diodes: Hole localization,
 Auger processes, and the green gap. Appl. Phys. Lett. 109,
 161103 (2016).
- J. Piprek, F. Romer, B. Witzigmann. On the uncertainty of the Auger recombination coefficient extracted from In-GaN/GaN light-emitting diode efficiency droop measurements. Appl. Phys. Lett. 106, 101101 (2015).
- K.T. Delaney, P. Rinke, C.G. Van de Walle. Auger recombination rates in nitrides from first principles. Appl. Phys. Lett. 94, 191109 (2009).
- F. Bertazzi, M. Goano, E. Bellotti. A numerical study of Auger recombination in bulk InGaN. Appl. Phys. Lett. 97, 231118, (2010).
- F. Bertazzi, M. Goano, E. Bellotti. Numerical analysis of indirect Auger transitions in InGaN. Appl. Phys. Lett. 101, 011111 (2012).
- E. Kioupakis, P. Rinke, K.T. Delaney, C.G. Van de Walle. Indirect Auger recombination as a cause of efficiency droop in nitride light-emitting diodes. *Appl. Phys. Lett.* 98, 161107 (2011).
- E. Kioupakis, D. Steiauf, P. Rinke, K.T. Delaney, C.G. Van de Walle. First-principles calculations of indirect Auger recombination in nitride semiconductors. *Phys. Rev. B* 92, 035207 (2015).
- A.V. Zinovchuk, A.M. Gryschuk. Alloy-assisted Auger recombination in InGaN. Opt. Quant. Electron. 50, 455 (2018).
- F. Bernardini, V. Fiorentini. Spontaneous versus piezoelectric polarization in III–V nitrides: Conceptual aspects and practical consequences. *Phys. Stat. Sol. B* 216, 391 (1999).
- J. Hader, J.V. Moloney, B. Pasenow, S.W. Koch, M. Sabathil, N. Linder, S. Lutgen. On the importance of radiative and Auger losses in GaN-based quantum wells. Appl. Phys. Lett. 87, 201112 (2005).
- R. Vaxenburg, A. Rodina, E. Lifshitz, A.L. Efros. The role of polarization fields in Auger-induced efficiency droop in nitride-based light-emitting diodes. *Appl. Phys. Lett.* 103, 221111 (2013).
- R. Vaxenburg, E. Lifshitz, and A.L. Efros. Suppression of Auger-stimulated efficiency droop in nitride-based light emitting diodes. Appl. Phys. Lett. 102, 031120 (2013).
- F. Bertazzi, X. Zhou, M. Goano, G. Ghione, E. Bellotti. Auger recombination in InGaN/GaN quantum wells: A full-Brillouin-zone study. Appl. Phys. Lett. 103, 081106 (2013).
- J.M. McMahon, E. Kioupakis, S. Schulz. Atomistic analysis of Auger recombination in c-plain (In,Ga)N/GaN quantum wells: Temperature-dependent competition between radiative and nonradiative recombination. *Phys. Rev. B* 105, 195307 (2022).

- D. Iida, Z. Zhuang, P. Kirilenko, M. Velazquez-Rizo, M.A. Najmi, K. Ohkawa. 633-nm InGaN-based red LEDs grown on thick underlying GaN layers with reduced in-plane residual stress. Appl. Phys. Lett. 116, 162101 (2020).
- D. Esseni, P. Palestri. Linear combination of bulk bands method for investigating the low-dimensional electron gas in nanostructured devices. *Phys. Rev. B* 72, 165342 (2005).
- D. Vasileska, S.M. Goodnick, G. Klimeck. Computational Electronics: Semiclassical and Quantum Device Modeling and Simulation (CRC Press, 2010).
- Z.H. Mahmood, A.P. Shah, A. Kadir, M.R. Gokhale, S. Ghosh, A. Bhattacharya, B.M. Arora. Determination of InNπïSGaN heterostructure band offsets from internal photoemission measurements. Appl. Phys. Lett. 91, 152108 (2007).
- P.Y Prodhomme, A. Beya-Wakata, G. Bester. Nonlinear piezoelectricity in wurtzite semiconductors. *Phys. Rev. B* 88, 121304(R) (2013).
- K. Adachi, H. Ogi, A. Nagakubo, N. Nakamura, M. Hirao, M. Imade, M. Yoshimura, Y. Mori. Elastic constants of GaN between 10 and 305 K. J. Appl. Phys. 119, 245111 (2016).
- J. Serrano, A. Bosak, M. Krisch, F.J. Manjon, A.H. Romero, N. Garro, X. Wang, A. Yoshikawa, M. Kuball. InN thin film lattice dynamics by grazing incidence inelastic X-ray scattering. *Phys. Rev. Lett.* 106, 205501 (2011).
- O. Bonno, J.L. Thobel, F. Dessenne. Modeling of electronelectron scattering in Monte Carlo simulation of quantum cascade lasers. J. Appl. Phys. 97, 043702 (2005).
- H. Haug S.W. Koch. Quantum Theory of the Optical and Electronic Properties of Semiconductors (World Scientific Publishing Co. Pte. Ltd., 2004).
- A. David, N.G. Young, C. Lund, M.D. Craven. Reduction of efficiency droop in c-plane InGaN/GaN light-emitting diodes using a thick single quantum well with doped barriers. Appl. Phys. Lett. 115, 193502 (2019).
- D. Schiavon, M. Binder, M. Peter, B. Galler, P. Drechsel, F. Scholz. Wavelength-dependent determination of the recombination rate coefficients in single-quantum-well GaInN/GaN light emitting diodes. *Phys. Status Solidi B* 250, 283 (2013).
- T.H. Ngo, B. Gil, B. Damilano, K. Lekhal, P. De Mierry. Internal quantum efficiency and Auger recombination in green, yellow and red InGaN-based light emitters grown along the polar direction. Superlatt. Microstruct. 2103, 245 (2017).
- C. Smith, R.A. Abram, M.G. Burt. Theory of Auger recombination in a quantum well heterostructure. Superlatt. Microstruct. 1, 119 (1985).
- R.I. Taylor, R.A. Abramz, M.G. Burt, C. Smith. A detailed study of Auger recombination in 1.3μm InGaAsP/InP quantum wells and quantum well wires. Semicond. Sci. Technol. 5, 90 (1990).

35. G.E. Cragg, A.L. Efros. Suppression of Auger processes in confined structures. $Nano\ Lett.\ {\bf 10},\ 313\ (2010).$

Received 28.04.25.

Translated from Ukrainian by O.I. Voitenko

А.В. Зіновчук, В.С. Сліпокуров

ОЖЕ-РЕКОМБІНАЦІЯ В ПОЛЯРНИХ InGaN/GaN КВАНТОВИХ ЯМАХ

Проведено розрахунок швидкості оже-рекомбінації в полярних квантових ямах ${\rm In}_x{\rm Ga}_{1-x}{\rm N}/{\rm Ga}{\rm N}$ на основі моделі повних енергетичних зон. Ключовими складовими розрахункової моделі були зонні структури об'ємних бінарних нітридів (GaN та InN), що отримувалися методом ємпіричного псевдопотенціалу, та зонні структури квантових ям

 ${\rm In}_x{\rm Ga}_{1-x}{\rm N}/{\rm Ga}{\rm N}$ (для різних x), що отримувалися методом лінійної комбінації об'ємних зон. Розраховано залежність коефіцієнтів оже-рекомбінації від ширини забороненої зони, товщини квантової ями та концентрації носіїв заряду. Результати розрахунку показують, що оже-коефіцієнти в квантових ямах набагато слабше залежать від ширини заборонної зони, ніж у випадку об'ємних ${\rm In}_x{\rm Ga}_{1-x}{\rm N}$ сполук. Залежність оже-коефіцієнтів від товщини ями має сильний осциляційний характер. При високих концентраціях носіїв заряду спостерігається значне спадання оже-коефіцієнтів, що є наслідком впливу статистики Фермі на розподіл носіїв заряду по квантових станах.

 $K\,n\,v\,v\,o\,s\,i\,$ $c\,n\,o\,s\,a$: In
GaN квантові ями, оже-рекомбінація, поляризація.